Manipulating Molecules via Combined Static and Laser Fields

Bretislav Friedrich* and Dudley Herschbach*

*Department of Chemistry and Chemical Biology, Harvard University, 12 Oxford Street,
Cambridge, Massachusetts 02138*

Received: June 24, 1999

Interaction of the strong electric field of an intense laser beam with the anisotropic polarizability of a linear molecule creates pendular states, superpositions of the field-free rotational states, in which the molecular axis librates about the field direction. Angular motion in the low-lying pendular states is thereby restricted by a double-well potential, governed by the laser intensity. The pendular energy levels occur as pairs of opposite parity, with separations corresponding to the frequency for tunneling between the wells. If the molecule is polar or paramagnetic, introducing a static electric or magnetic field connects the nearly degenerate pendular levels and thus induces strong pseudo-first-order Stark or Zeeman effects. This can be exploited in many schemes to control and manipulate molecular trajectories.

1. Introduction

The pursuit of means to manipulate molecular trajectories and reaction pathways is now a leading frontier of chemical physics. With roots reaching back to the venerable state-selection methods of Stern[1] and Rabi,[2] the modern incarnation of this pursuit relies chiefly on pulsed laser techniques.[3–5] A recent seminal achievement is the use of iterative feedback, guided by optimal control theory, to enable molecules to teach experimenters how best to tailor light pulses to maximize the desired effect.[6,7] Among other developments are methods for controlling the rotational orientation or alignment[8,9] of molecules and for deflecting or focusing the translational motion.[10,11]

All schemes for manipulating gas phase molecules face a fundamental difficulty. For neutral molecules, the interactions of permanent or induced dipole moments with static or laser fields are typically quite weak compared with the rotational and translational kinetic energy. The profusion of molecular vibrational and rotational levels thwarts laser-cooling techniques that are very effective for atoms.[12] Accordingly, proposed strategies for manipulating molecular trajectories often must invoke special properties of particular molecules. In this paper, we consider a rather general approach, amenable to a wide variety of molecules and applications. The key aspect is a means to endow a polar or paramagnetic molecule, in certain of its low-lying rotational states, with a strong pseudo-first-order Stark or Zeeman effect. Such molecules, whether linear or asymmetric, in effect can be made to act almost like a symmetric top. The enhanced interaction with external fields provided thereby can be exploited in many methods designed to control or restrict molecular orientation or translation.

The pseudo-first-order effects arise from the combined action of a static electric or magnetic field and an intense nonresonant laser field. In previous work, we have analyzed for linear molecules the action of such fields, considered separately.[13] Each gives rise to low-lying pendular states, coherent superpositions or hybrids of the field-free rotational states, in which the molecular axis librates over a limited angular range about the field direction. There are, however, marked differences between the static field case, which involves interaction with a permanent electric or magnetic dipole, and the nonresonant laser case, which involves an induced dipole arising from the molecular polarizability.

In section 2, we evaluate energy levels and wave functions for a linear molecule subject to collinear static and nonresonant laser fields, in the adiabatic regime wherein the fields are turned on and off slowly compared with rotational periods. We examine particularly how the level shifts and spatial distribution of the molecular axis depend on dimensionless parameters characterizing the strength of the interactions with the static and laser fields. In section 3, we treat in detail the pseudo-first-order effects. These arise because the induced dipole interaction produces a double-well potential, governed by the anisotropy of the polarizability and the laser intensity. The pendular energy levels thus occur as tunneling doublets. If the molecule is polar or paramagnetic, introducing a static electric or magnetic field connects the nearly degenerate pairs of pendular levels. Thus, often even a very weak static field can convert second-order alignment by a laser into a strong first-order orientation. In section 4 we assess parameters for representative molecules and discuss a few prospective applications.

2. Pendular States in Collinear Static and Laser Fields

We consider a $^1\Sigma$ molecule, treated as a rigid rotor with a permanent dipole μ along the internuclear axis and polarizability components $\alpha_{||}$ and $\alpha_{\perp}$ parallel and perpendicular to the axis. It is subjected to a static electric field, ε_S, which is collinear with the electric vector of a plane-polarized laser field, $\varepsilon_L(t)$. By virtue of the azimuthal symmetry about the collinear fields, the interaction potentials, V_μ and V_α, involve just the polar angle θ between the molecular axis and the field direction. Likewise, the projection M on the field direction of the rotational angular momentum vector $\mathbf{J}$ is a constant of the motion, or "good" quantum number. This is taken into account in the usual way,[13] which introduces into the Hamiltonian an M-dependent scalar centrifugal potential.

We limit consideration to a pulsed laser field,

$$\varepsilon_L{}^2(t) = 2I_\text{o}\text{g}(t/\tau)\cos^2(2\pi\nu t) \qquad (1)$$

where I_o denotes the peak intensity and $\text{g}(t/\tau)$ the pulse time profile, with τ the pulse duration. The oscillation frequency ν

Manipulating Molecules via Static and Laser Fields

J. Phys. Chem. A, Vol. 103, No. 49, 1999 **10281**

is far removed from any molecular resonance and much higher than both $1/\tau$ and rotational periods. The Hamiltonian $H(t)$ thus is averaged over these rapid oscillations, which quenches interaction of the permanent dipole with $\varepsilon_L(t)$ and reduces the time dependent factor in the polarizability interaction to

$$\langle e\varepsilon_L^2(t)\rangle_\nu = I_L(t) = I_o g(t/\tau) \tag{2}$$

We will examine instantaneous eigenstates pertinent to the adiabatic regime, in which the pulse is turned on and off slowly compared with the rotational periods. In this regime, the time evolution of the pendular states faithfully follows the field as if it were static at any instant, despite the strong intensity of the laser pulse. Accordingly, the instantaneous pendular eigenstates depend only parametrically on the pulse profile. A criterion for adiabatic behavior, $\tau > 5\hbar B$, with B the molecular rotational constant, has been demonstrated computationally for a Gaussian pulse.[14] Recently, an elegant YAG-Laser experiment on the alignment of iodine has confirmed that the alignment indeed tracks the pulse profile as the field-free rotational states evolves into pendular states and then back into field-free states.[15]

Hamiltonian and Interactions. With the oscillatory time-dependence averaged out, the pulse time-dependence incorporated in an adiabatic parameter, and energies expressed in units of the rotational constant B, the Hamiltonian takes the form

$$H = -\frac{d^2}{d\theta^2} + V_{eff}(\theta) \tag{3}$$

which describes one-dimensional motion in the polar angle θ, subject to an effective potential

$$V_{eff}(\theta) = \left[\frac{M^2 - \frac{1}{4}}{\sin^2\theta} - \frac{1}{4}\right] + V_\mu + V_\alpha \tag{4}$$

This displays explicitly the centrifugal term, which for $|M| > 0$ provides a repulsive contribution competing with the permanent and induced dipole interactions. The interaction potentials are

$$V_\mu(\omega; \theta) = -\omega\cos\theta, \tag{5}$$

$$V_\alpha(\omega_\parallel, \omega_\perp; \theta) = -(\Delta\omega\cos^2\theta + \omega_\perp) \tag{6}$$

with dimensionless parameters defined by

$$\omega = \mu\varepsilon_S/B \tag{7}$$

$$\Delta\omega = \omega_\parallel - \omega_\perp \tag{8}$$

$$\omega_{\parallel,\perp} = \frac{1}{2}\alpha_{\parallel,\perp}I_L/B \tag{9}$$

where $I_L(t)$ comes from eq 2. Since the term $\omega_\perp$ in eq 6 enters as an additive constant, it is convenient to use a reduced energy quantity,

$$\lambda = E/B + \omega_\perp \tag{10}$$

where E is the usual eigenenergy. This merely shifts the zero of energy to $-\omega_\perp$ with respect to the ground state of the field-free rotor.

The same expressions hold if ε_S is replaced by a static magnetic field, H_S, in the case of $\Omega = 0$ states of a linear molecule.[16,17] However, since in any paramagnetic electronic

state the magnetic moments μ_m and $-\mu_m$ occur with equal probability, the corresponding dimensionless parameter

$$\omega_m = \mu_m H_S/B \tag{11}$$

takes on both positive and negative values. Reversing the sign of ω does not change the eigenenergies but is equivalent to shifting by 180° the cosine potential of eq 7; consequently, the expectation value of the orientation cosine, $\langle\cos\theta\rangle$, reverses sign if ω does. For simplicity, here we omit consideration of $\Omega \neq 0$ states, but the modifications needed for these can be readily incorporated as in previous treatments dealing with H_S alone[16] or parallel H_S and ε_S fields.[17]

In evaluating eigenproperties for eq 3, as in previous treatments dealing with either ε_S, H_S, or $\varepsilon_L(t)$ alone, it is natural and efficient to set up secular equations by expanding the wavefunctions in spherical harmonics, $Y_{JM}(\theta,\phi)$, the field-free eigenfunctions. Solutions are obtained by straightforward, standard methods. The pendular eigenfunctions,

$$\Psi = \Sigma_J c_{\tilde{J};J,M}(\omega,\Delta\omega)Y_{JM}(\theta,\phi) \equiv |\tilde{J},M; \omega,\Delta\omega\rangle \tag{12}$$

and hybridization coefficients $c_{\tilde{J};J,M}(\omega,\Delta\omega)$ are labeled with a nominal $\tilde{J}$ symbol which designates the value of J for the field-free rotor state that adiabatically correlates with the hybrid pendular state. Since M is a good quantum number, its value remains the same for all the field-free states contributing to any given pendular state. The range of J that enters this coherent superposition increases with the ω and $\Delta\omega$ parameters. If only the V_α interaction is present, the hybrids involve either even J or odd J contributions only, for any fixed M, so the resulting wavefunctions have definite parity, given by $(-1)^J$. When V_μ is present, both even and odd J terms enter, and the wavefunctions then have no definite parity.

Effective Potentials and Eigenproperties. Figure 1 illustrates aspects typical when the induced dipole interaction is modest ($\Delta\omega = 50$) but substantially stronger than the permanent dipole interaction ($\omega = 10$). For the laser field alone ($\omega = 0$, dashed curves), the V_{eff} functions are symmetric double well potentials, with the equivalent minima shifting to wider angles away from the poles (at $\theta = 0°$ and 180°) as $|M|$ increases, thereby adding centrifugal repulsion. Turning on the static field (full curves)skews the V_{eff} functions to favor angles closer to the field ($\theta = 0°$), since the permanent dipole interaction is attractive for $\theta < 90°$ but repulsive for $\theta > 90°$. With the static field off, the bound energy levels (dashed) all consist of close tunneling doublet pairs: e.g., (0,0; 1,0) and (2,0; 3,0) for the $|M| = 0$ case. With the static field on, these pairs are strongly split apart, with the levels (full lines) shifting roughly symmetrically with respect to the field-off (dashed) positions. This exemplifies the process to be discussed in section 3, which produces pseudo-first-order behavior. For the various pendular states, the orientation or alignment attained is also indicated by noting (with diamonds or dots) the angles corresponding to $\langle\cos\theta\rangle$ or $\langle\cos^2\theta\rangle$, respectively.

Figure 2, with the same format, shows the situation when the permanent dipole and induced dipole interactions are comparable ($\Delta\omega = \omega = 10$) but rather weak, capable of binding only a couple of levels for $|M| = 0$ or 1. The skewing introduced by V_μ is now much more pronounced and the splitting of the tunneling doublets is quite asymmetrical. This serves to emphasize that varying $\Delta\omega$ and ω gives rise to a wide range of properties.
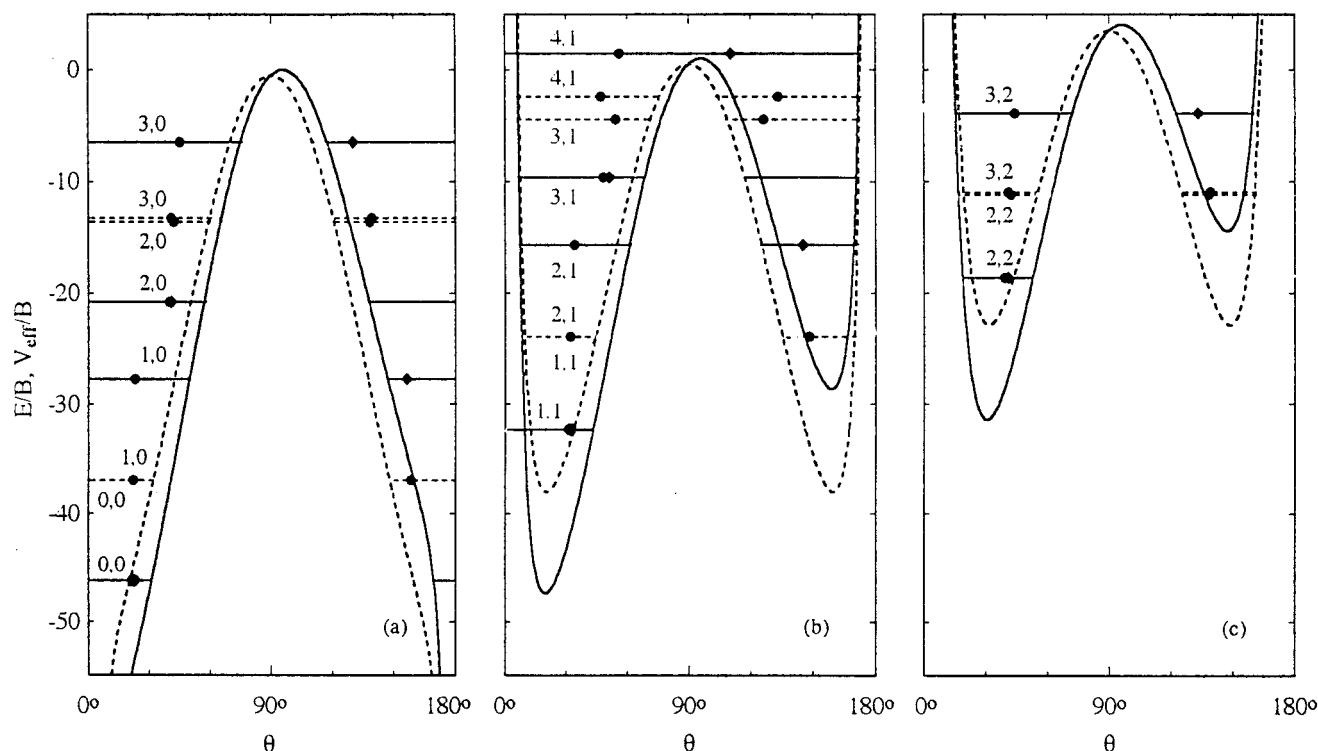
Figure 1. Effective potentials for (a) $M = 0$, (b) $M = 1$, and (c) $M = 2$ for a laser field with $\Delta\omega = 50$. Potential curves and pendular energy levels are shown both with a collinear static electric field present ($\omega = 10$, full curves) and absent ($\omega = 0$, dashed curves). Energies are in units of the rotational constant; the zero of energy is at $-\omega_\perp$ with respect to the field-free limit. Levels are labeled J,M where J denotes the value of J for the field-free rotor state that correlates adiabatically with the hybrid pendular state. Dots indicate angles that correspond to the alignment parameter, $\langle\cos^2\theta_L\rangle$; diamonds indicate angles corresponding to the orientation parameter $\langle\cos\theta_S\rangle$.
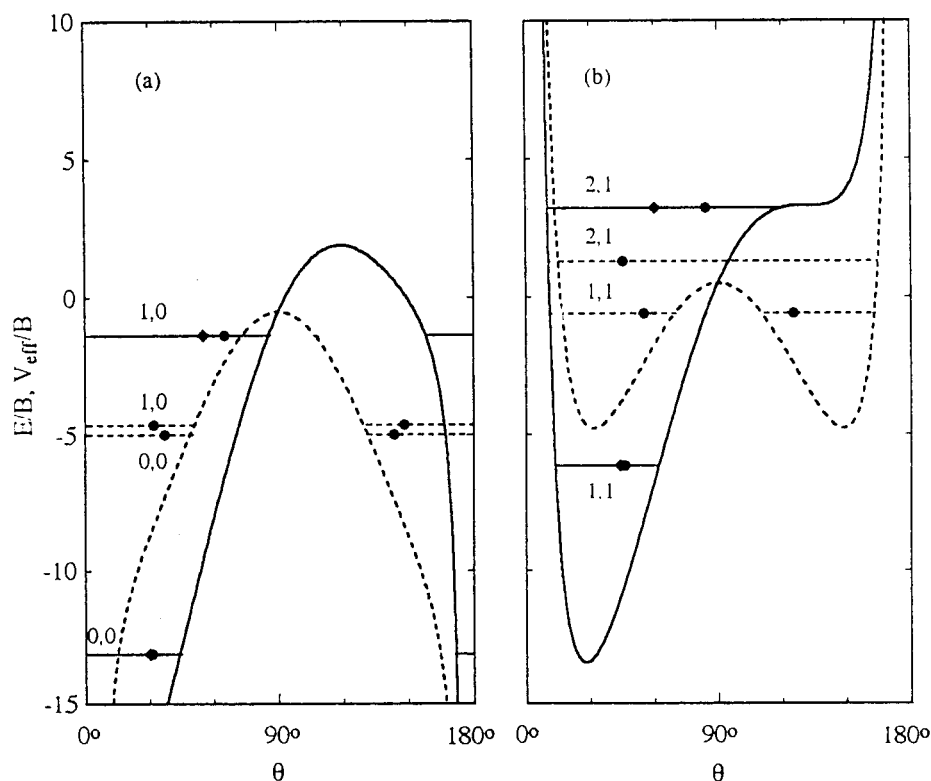

Figure 2. Effective potentials for (a) $M = 0$ and (b) $M = 1$ for a laser field with $\Delta\omega = 10$. Potential curves and pendular energy levels are shown both with a collinear static electric field present ($\omega = 10$, full curves) and absent ($\omega = 0$, dashed curves). Other aspects as in Figure 1.

Figures 3 and 4 provide a broader view of distinctive features of the permanent and induced dipole interactions, as manifested in the low-lying pendular energy levels and their directional propensities. For both interactions, singly or together, the lowest pendular state (0,0) moves steadily downward as the field strength increases; it is always a "high field seeking" state. When only V_μ is present, however, the net interaction is initially repulsive for some states (Figure 3a, for $M/J < \frac{1}{3}$); these are

Manipulating Molecules via Static and Laser Fields

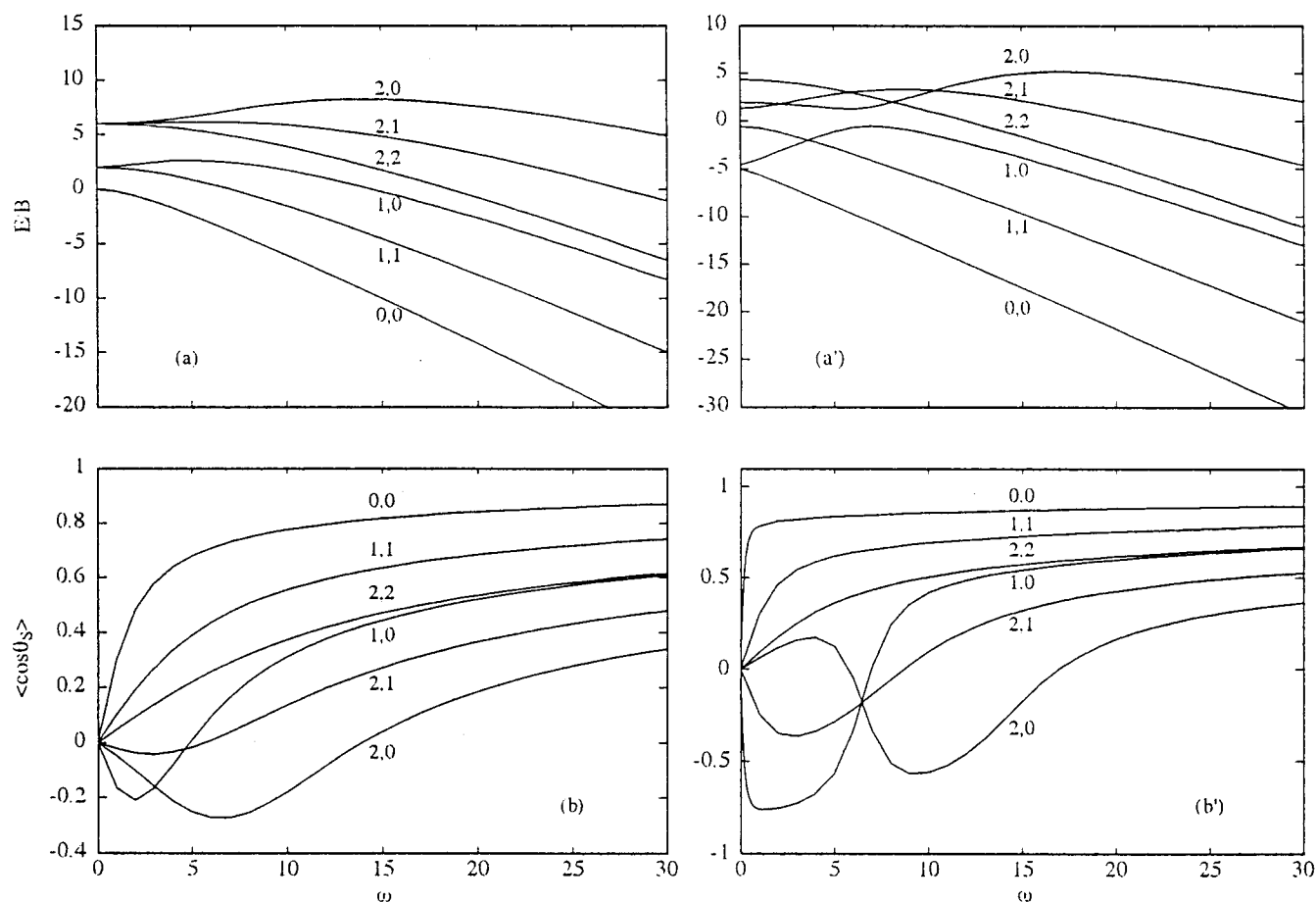*J. Phys. Chem. A, Vol. 103, No. 49, 1999* **10283**

Figure 3. Variation with permanent dipole interaction parameter ω of the (a) pendular energy levels and (b) orientation cosine $\langle\cos\theta_S\rangle$, with laser field absent ($\Delta\omega = 0$) or (a′) and (b′) with it present ($\Delta\omega = 10$). Pendular states labeled as in Figure 1.

"low-field seeking" states. If the static field becomes sufficiently strong to enable V_{eff} to bind well such a state, thereafter its energy moves downward and it also becomes a high field seeking state. When only V_α is present, the interaction is purely attractive for all states (Figure 4a), so regardless of the field strength all are high-field seeking states. Moreover, as already noted, the levels pair up as tunneling doublets ($\tilde{J},M;\tilde{J}+1,M$), the more so as the field strength increases.

When both V_μ and V_α are present, the most striking new features of the energy levels (Figures 3a′, 4a′) arise from the splitting of the tunneling doublets. This also induces level crossings and avoided intersections. For instance, as $\Delta\omega$ increases, with $\omega = 10$ (Figure 4a′), the 2,0 level, which is the lower component of a tunneling doublet, is increasingly "repelled" from the upper component, the 3,0 level, and descends rapidly in energy. The 2,0 level thus undergoes genuine crossings with the 2,1 and 2,2 levels, with which it does not interact because these have different values of M, but suffers an avoided intersection with the 1,0 level, with which it mixes because the value of M is the same.

The directional properties of the pendular states are readily derived from the eigenenergies via the Hellmann−Feynman theorem. Expectation values characterizing the extent of orientation or alignment thus are given by

$$\langle\cos\theta\rangle = -\partial\lambda/\partial\omega \quad \text{and} \quad \langle\cos^2\theta\rangle = -\partial\lambda/\partial(\Delta\omega) \quad (13)$$

respectively. When only V_μ is present (Figure 3b), the molecular axis is oriented toward the field, the "right way," for high-field seeking states ($\langle\cos\theta\rangle > 0$) and the "wrong way" for low-field seeking states ($\langle\cos\theta\rangle < 0$), such as 1,0. The latter orientation

occurs whenever the dipole continues to pinwheel, with its plane near the field direction, since then the dipole speeds up as it swings toward the field and slows down as it retreats. However, right-way orientation emerges when the field becomes strong enough to convert pinwheeling into pendular motion. When only V_α is present (Figure 4b), the pendular states are not oriented ($\langle\cos\theta\rangle = 0$) but only aligned with respect to the double-ended electric field. Here, for states pinwheeling above the attractive potential, there occurs what could be termed "wrong-way alignment," in which the molecular axis points predominately perpendicular to the laser field ($\langle\cos^2\theta\rangle < 1/3$). Again, "right-way alignment," favoring the field direction, emerges once the field becomes strong enough to draw the state well down into the potential well and thereby confine the molecular axis to librational motion.

The combined fields produce marked variations in $\langle\cos\theta\rangle$ and $\langle\cos^2\theta\rangle$ for certain states (Figures 3b′, 4b′). For close tunneling doublets, such as (0,0; 1,0), even a very weak static field can result in quite strong orientation, with $\langle\cos\theta\rangle$ large and positive for the lower energy component (0,0) and equally large but negative or wrong-way for the higher energy component (1,0). Yet, even for such cases, a sufficiently strong static field can impose right-way orientation on the higher energy component (as for the 1,0 state in Figure 3b′). Avoided intersections likewise can introduce abrupt directional changes (as for the 1,0 and 2,0 states in Figure 4b′).

Similar features appear for $\Omega = 0$ states if the static field is magnetic, but the equivalence of $\pm\omega$ is tantamount to making the static field double-ended, so the molecular axis cannot be oriented but only aligned.
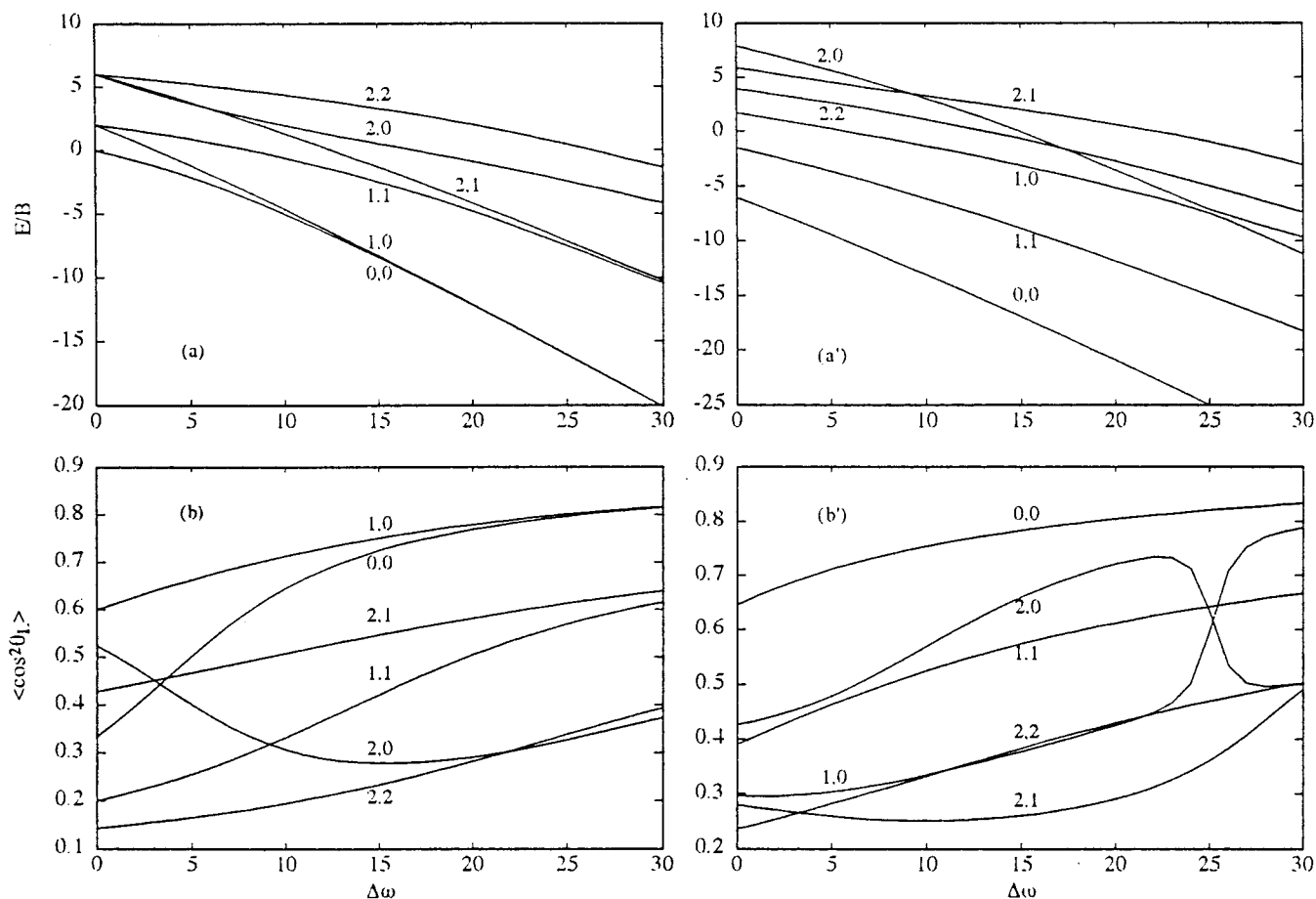
Figure 4. Variation with induced dipole interaction parameter $\Delta\omega$ of the (a) pendular energy levels and (b) alignment squared cosine $\langle\cos^2\theta_L\rangle$, with static field absent ($\omega = 0$) or ((a') and (b') with it present ($\omega = 10$). Pendular states labeled as in Figure 1.

TABLE 1: Tunneling Doublets Produced by V_α Potential[a]

$J, |M| - J+1, |M|$	a	b	$\Delta\omega^*$
0,0−1,0	3.6636	2	3
1,1−2,1	6.7912	1.95	12
2,0−3,0	8.9619	1.79	25
2,2−3,2	11.0186	2.12	30
3,1−4,1	13.2708	1.98	44
3,3−4,3	20.9856	3.23	55

[a] Parameters a and b pertain to eq 14. A given pair of levels, $J, |M|$; $J+1, |M|$ becomes bound in the V_α double-well potential when the anisotropy parameter of eq 8 exceeds the value $\Delta\omega^*$.

3. Pseudo-First-Order Stark and Zeeman Effects

The $\cos^2\theta$ potential is not among textbook examples of symmetric double-well potentials, but deserves to be, since solutions can be determined exactly from an oblate spheroidal wave equation.[13,19] To a good approximation, the tunneling splittings can be obtained from an elementary semiclassical treatment.[18] Table 1 lists for the lowest six pairs of doublet levels the minimum value of $\Delta\omega$ required to bind both members of each pair. For these doublets the exact splittings are found to be well represented by

$$\Delta\lambda_0/\lambda_0 = \exp(a - b\sqrt{\Delta\omega}) \quad (14)$$

The subscript indicates $\omega = 0$. The listed values of the coefficients a and b were fitted to data from ref 19; the formula is accurate to about 5% or better as long as both members of the doublet are bound states. In applications, $\Delta\omega$ is typically large enough that the eigenenergy λ_0 can be well approximated by analytic expressions for the high-field limit.[13]

Two-State Model. A simple two-state model for the pseudo-first order interaction is useful for heuristic purposes or quick estimates. When $\omega = 0$, the wave functions for the upper and lower components of a tunneling doublet,

$$\Psi_U \equiv |\tilde{J}+1,M;0,\Delta\omega\rangle \text{ and } \Psi_L \equiv |\tilde{J},M;0,\Delta\omega\rangle$$

are of opposite parity. In Ψ_U, the contributing spherical harmonics all have J either even or odd; in Ψ_L, vice versa. Since the permanent dipole interaction has indefinite (or mixed) parity, it introduces a coupling matrix element,

$$-\omega Z_{UL} \equiv \omega\langle\Psi_U|\cos\theta|\Psi_L\rangle$$

The eigenenergies $\lambda_\pm$ and wave functions $\Psi_\pm$ are then given by

$$\lambda_\pm = \frac{1}{2}(\lambda_U + \lambda_L) \pm \frac{1}{2}[(\Delta\lambda_0)2 + 4\omega^2 Z_{UL}{}^2]^{1/2} \quad (15)$$

$$\begin{pmatrix}\Psi_+\\\Psi_-\end{pmatrix} = \begin{pmatrix}\cos\chi & \sin\chi\\-\sin\chi & \cos\chi\end{pmatrix}\begin{pmatrix}\Psi_U\\\Psi_L\end{pmatrix} \quad (16)$$

with the mixing angle determined by

$$\tan 2\chi = |2\omega Z_{UL}|/\Delta\lambda_0 \quad (17)$$

Since even for small ω the $\lambda_\pm$ levels may split apart so strongly as to trespass on others (cf. Figures 4a and a'), the two-state model can only serve as a rough guide. However, we find that the effect of perturbations by other states can be simulated fairly well by a simple expedient. This involves inverting eq 15 and

Manipulating Molecules via Static and Laser Fields

J. Phys. Chem. A, Vol. 103, No. 49, 1999 **10285**

TABLE 2: Parameters for Two-State Model[a]

$\Delta\omega$	ω	$\Delta\lambda$	χ	$|Z_{10}|$	$|\langle\cos\theta\rangle|$	$\langle\cos\theta\rangle_{0,0}$	$\langle\cos\theta\rangle_{1,0}$
10	0	0.369					
	0.1	0.402	11.6°	0.796	0.315	0.316	−0.315
	1	0.632	38.5°	0.795	0.774	0.786	−0.760
	10	11.765	44.1°	0.588	0.795	0.852	0.421
20	0	0.063					
	0.1	0.184	35.0°	0.870	0.818	0.817	−0.816
	1	1.740	44.0°	0.869	0.869	0.872	−0.866
	10	15.795	44.9°	0.750	0.869	0.890	0.522
50	0	0.001					
	0.1	0.185	44.8°	0.923	0.923	0.923	−0.923
	1	0.846	45.0°	0.923	0.923	0.924	−0.923
	10	18.458	45.0°	0.923	0.923	0.928	−0.917

[a] For the lowest tunneling doublet (0,0; 1,0). Splittings $\Delta\lambda$ are differences of eigenenergies of eq 10. Nominal values of coupling matrix element Z_{10} derived from splittings via eq 15, mixing angle χ for eigenfunctions from eq 16. Expectation value of orientation cosine, $\langle\cos\theta\rangle$, from eq 17; exact results computed from eigenfunctions of eq 12 are given for comparison.
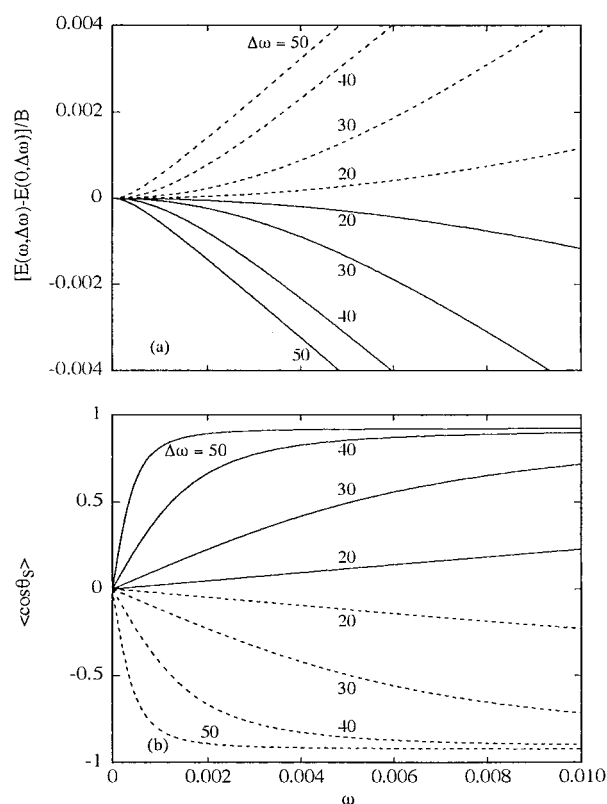

Figure 5. Effect of combined action of collinear static and laser fields on (a) shift of energy levels relative to those with static field absent and (b) expectation value $\langle\cos\theta_S\rangle$ of orientation cosine, for the $J, M =$ 0,0 (full curves) and 1,0 states (dashed curves). Curves show variation with ω, the strength of the permanent dipole interaction (here very weak), for several values of $\Delta\omega$, the strength of the induced dipole interaction. For $\omega = 0$, and $\Delta\omega > 3$, the 0,0 and 1,0 states are components of a tunneling doublet and become nearly degenerate as $\Delta\omega$ increases. When $\omega \neq 0$ these levels split apart strongly and thus acquire large effective dipole moments, opposite in sign. Thereby the molecular axis becomes oriented, in the 0,0 state parallel to the static field and in the 1,0 state antiparallel.

fitting nominal values of the coupling matrix element Z_{UL} to accurately calculated values of $\Delta\lambda_{\pm} \equiv \lambda_+ - \lambda_-$; thereby, Z_{UL} becomes a function of ω as well as $\Delta\omega$. The expectation values of the orientation cosines for the $\Psi_{\pm}$ states can then be estimated from

$$\langle\Psi_{\pm}|\cos\theta|\Psi_{\pm}\rangle = \mp|Z_{\text{UL}} + \omega\partial Z_{\text{UL}}/\partial\omega|\sin2\chi \quad (18)$$
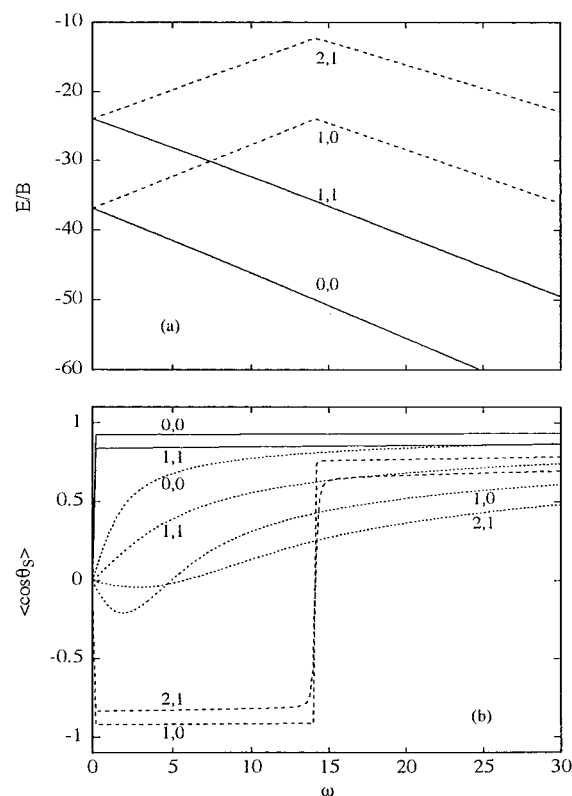

Figure 6. Variation with permanent dipole interaction parameter ω of (a) energy levels when $\Delta\omega = 50$ and (b) orientation cosine when $\Delta\omega = 0$ and 50. Results are shown for two tunneling doublets: the 0,0 (full curves) and 1,0 states (dashed) and the 1,1 (full) and 2,1 states (dashed). In contrast to Figure 5, for $\Delta\omega = 50$ at the large values of ω shown here the Stark effect has become fully first order. In (a), the level shifts thus simply increase linearly with ω, until about $\omega \approx 17$, where those for the 1,0 and 2,1 states are abruptly reversed by intesections with higher-lying states (2,0 and 3,1 respectively). In (b), this reversal produces a corresponding abrupt switch in the orientation direction for the 1,0 and 2,1 states (cf. Figures 7 and 8). The $\Delta\omega = 0$ curves (dotted) are included to show the orientation due to the permanent dipole alone.

Table 2 illustrates the two-state model for the lowest doublet. As expected, it works best when ω is small and $\Delta\omega$ large. In particular, when the splittings become markedly asymmetric (as in Figure 2), eq 18 fails badly for the upper component, although it still may give fairly good results for the lower state.

Figure 5 exhibits the typical behavior in the regime of nicely symmetrical splittings. The curves shown were obtained from exact solutions but are well simulated by the two-state model (with nominal Z_{UL}). In eq 15, the small size of $\Delta\lambda_0$, shrinking rapidly as $\Delta\omega$ increases, enables even a very weak static field to produce quite strong orientation, with $\langle\cos\theta\rangle$ large and positive for the lower member of the doublet state and equally large but negative for the upper member. Such a dramatic Stark effect resembles what occurs with l-type doublets of linear molecules in excited bending vibrational states or asymmetry doublets of near-symmetric top molecules.[20]

Figure 6 ilustrates a contrasting regime. For $\Delta\omega = 50$ and large values of ω, the Stark (or Zeeman) effect for both the lowest two pairs of doublet states has become fully first order, in accord with the two-state model. The level shifts simply increase linearly with ω, until about $\omega \approx 17$, where those for the each of the upper components are abruptly reversed by intersections with higher lying states. This reversal produces a corresponding abrupt switch in the orientation direction for the upper components. However, as seen by comparison with the
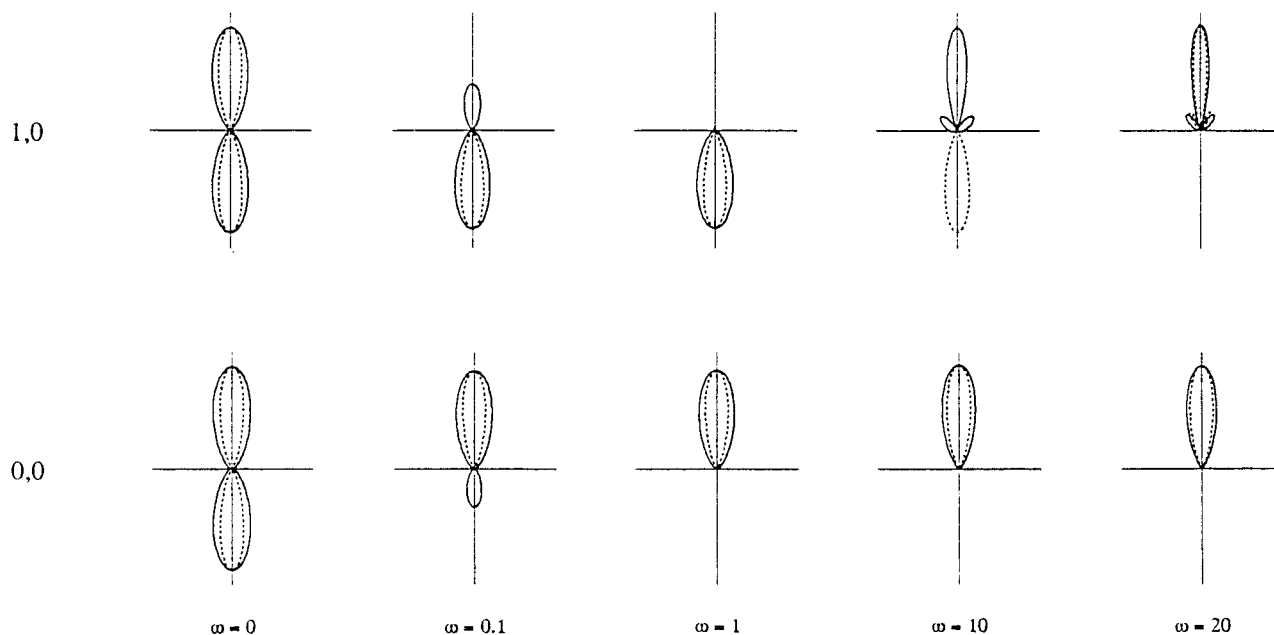
Figure 7. Polar plots of the wave functions for the pendular states 0,0 and 1,0 stemming from the tunneling doublet involved in the pseudo-first order Stark effect. Phases (not shown) are described in text. For $\Delta\omega = 10$ (full curves) and $\Delta\omega = 50$ (dotted curves) and values of ω ranging from 0 to 20. The direction of the collinear fields is vertical.
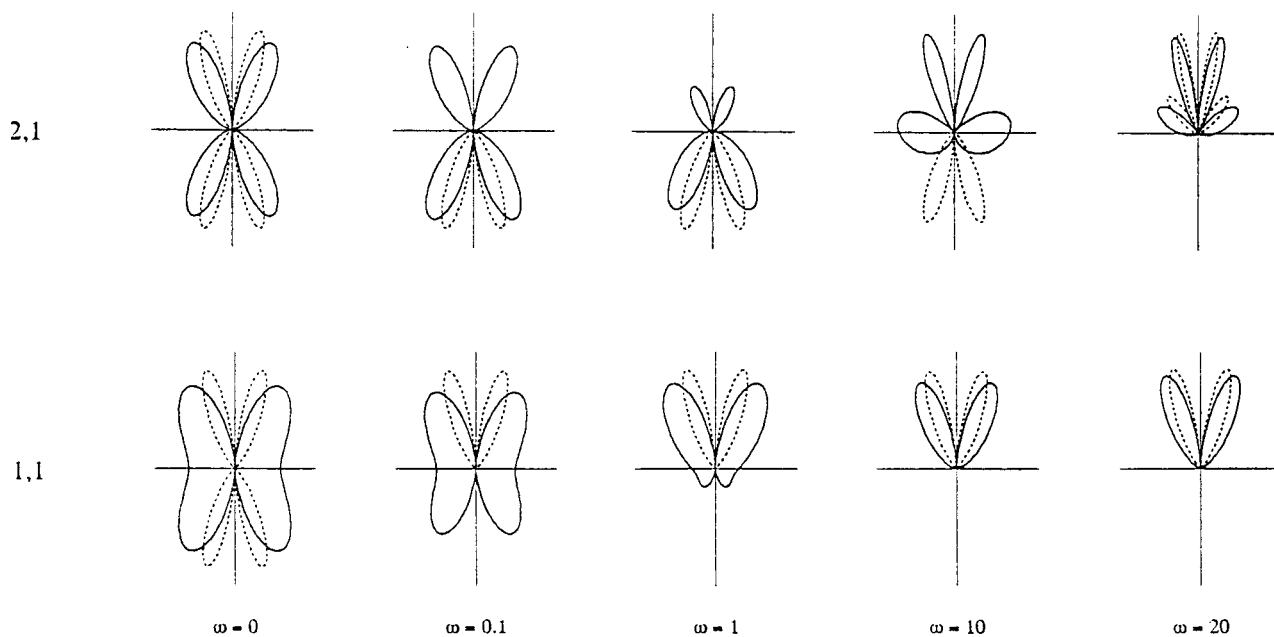

Figure 8. Polar plots of the wave functions for 1,1 and 2,1 pendular states, as in Figure 7.

$\Delta\omega = 0$ curves (dotted), the enhancement of orientation by the induced dipole interaction becomes only modest when the permanent dipole interaction is already large.

Evolution of Pendular Hybrids. Figure 7 displays how the form and directionality of the wave functions for the lowest doublet pair of states change as the V_α potential is augmented by addition of the V_μ potential. The field direction is vertical, and the polar plots, shown for $\Delta\omega = 10$ (full curves) and $\Delta\omega = 50$ (dotted), are normalized to unit amplitude. In the absence of V_μ, the 0,0 state has even parity (thus uniform phase), the 1,0 state odd parity (opposite phases for the two lobes of its wave function) but otherwise the form of both wave functions is the same. Turning on V_μ, even just with $\omega = 0.1$, converts the initial alignment into the characteristic, oppositely directed orientations. However, for both states, part of the probability distribution remains contrary to the dominant lobe. At $\omega = 1$,

the contrary portions have disappeared. By $\omega = 10$, the orientation of the 1,0 state has flipped to the "right way" when $\Delta\omega = 10$ (cf. Figure 2) but it remains the "wrong way" at $\Delta\omega = 50$ (cf. Figure 1). Finally, by $\omega = 20$, and spurred by admixture of the lower component of a higher doublet (cf. Figure 6), the 1,0 state has capitulated and becomes even more sharply oriented along the static field than is the 0,0 state.

Figure 8 traces the analogous ascent of the components of the 1,1; 2,1 doublet. With V_μ absent, for $\Delta\omega = 10$ the upper state 2,1 lies above the $\cos^2\theta$ barrier (cf. Figure 2) and its four-lobed wave function is distinctly less hybridized than that for the 1,1 state. At $\Delta\omega = 50$, however, the wave functions have assumed the same form for both states, aside from their parity (even for 2,1; odd for 1,1). When V_μ is turned on, the growth of orientation proceeds, again more rapidly for the lower component of the doublet. By $\omega = 20$ both states are fully

Manipulating Molecules via Static and Laser Fields

J. Phys. Chem. A, Vol. 103, No. 49, 1999 **10287**

directed into the hemisphere favored by the static field, although the centrifugal repulsion for $|M| = 1$ (cf. Figure 2) keeps the wave function lobes from lining up directly along the static field.

4. Prototypical Applications

Pendular hybridzation by a static field acting on a polar or paramagnetic molecule has proved a convenient means to produce oriented molecules for study of vector correlations in collision processes,[8,21] photodissociation,[22] and spectra.[23-25] It complements a more venerable but less general method, which provides oriented beams in pure rotational states but works only for symmetric top molecules and requires use of long ($\sim$1 m) inhomogeneous focusing fields.[26] The hydridization method is applicable to linear and asymmetric tops also and its experimental implementation merely requires installing a short ($\sim$1 cm) pair of parallel electrodes or pole pieces.

The kindred version of hybridization by the polarizability interaction, applicable to nonpolar as well as dipolar molecules, has likewise found several applications, both in spectroscopy[27] and in focusing[11] or aligning[15] neutral molecules by means of an intense nonresonant nanosecond laser pulse.

Many of these applications can be enhanced by creating doubly hybridized states via combined action of static and laser fields. The experimental implementation is easy, as the static field need extend only over the focal spot size of the laser. Particularly inviting is the opportunity to exploit the pseudo-first order Stark or Zeeman effect. This is not limited to linear molecules, but can be induced whenever anisotropy of the polarizability tensor creates an angular double-well potential. For instance, the exceptionally strong orientation produced by the pseudo-first-order interaction may enable state selection of the pendular states arising from the tunneling doublets, filtering them out from all the other much less strongly oriented states. A major limitation is that the orientation persists only for the duration of the pulse. Yet a nanosecond pulse is amply long to enable picosecond or femtosecond experiments with the oriented molecules.

Here we briefly assess specific prospects for a few molecules and applications that serve to illustrate new possibilities offered by the use of combined fields. With quantities expressed in customary practical units,

$$\Delta\omega = 10^{-11}\Delta\alpha(\text{Å}^3)I_{\text{L}}(\text{W/cm}^2)/B(\text{cm}^{-1}) \quad (19)$$

$$\omega = 0.0168\mu(\text{debye})\varepsilon_{\text{S}}(\text{kV/cm})/B(\text{cm}^{-1}) \quad (20)$$

or, in the magnetic case

$$\omega_\mu = 0.467\,\mu_{\text{m}}(\text{bohr magnetons})H_{\text{S}}(\text{tesla})/B(\text{cm}^{-1}) \quad (21)$$

As a standard for quick comparisons, we take $I_{\text{L}} = 10^{12}$ W/cm^2; pulsed lasers, even in the nanosecond range, can deliver considerably higher intensities, but some restraint is necessary to avoid ionizing the target molecule. Likewise, we usually take as standard $\varepsilon_{\text{S}} = 30$ kV/cm, although static electric fields two[25] and even four[28] times higher have been used in recent work without dire sparking. For the magnetic standard, we use $H_{\text{S}} = 1$ tesla, although fields several tenfold higher can be had (with no troubles from sparking). With these choices, ω for an electric dipole of 1 debye is about equal to ω_{m} for a magnetic moment of 1 bohr magneton. Table 3 lists parameters for a sampling of linear molecules, spanning a wide range in the interaction strengths.[20,29,30]

TABLE 3: Parameters for Representative Linear Molecules[a]

molecule	B [cm^{-1}]	μ [D]	$\Delta\alpha$ [Å^3]	ω [30kV/cm]	$\Delta\omega$ [10^{12}W/cm^2]
CsF	0.1843	7.87	(3.0)	21.5	160
KC*l*	0.1286	10.48	(3.1)	41.1	240
IC*l*	0.1142	1.24	(9.0)	5.5	800
DC*l*	5.445	1.18	0.74	0.11	2
DI	3.253	0.38	1.69	0.06	7
NO	1.703	0.16	2.8	0.05	6
CO(x$^1\Sigma^+$)	1.931	0.10	1.0	0.03	5
CO(a$^3\Pi$)	1.681	1.37	(1.5)	0.41	9
N$_2$O	0.4190	0.166	2.8	0.20	67
OCS	0.2039	0.709	4.1	1.75	200
C*l*CN	0.1990	2.80	(3.6)	7.09	180
ICN	0.1075	3.72	(7)	17.4	650
HCN	1.482	3.00	2.0	1.02	14
HCCC*l*	0.1067	0.44	4.1	2.1	380
HCCCN	0.1516	3.60	6.0	12.0	400

[a] Rotational constant B and dipole moments μ from refs 20 and 30. Polarizability anisotropies $\Delta\alpha$ mostly from data or bond polarizabilities given in ref 30. Values in parentheses estimated[29] from total polarizability using $\Delta\alpha/\alpha \approx 0.75$.

Alkali Halides. Despite unusually large dipole moments, orientation of molecules such as CsF and KCl is severely handicapped because high temperatures are required to vaporize them, so low-lying rotational states are sparsely populated. Adding a laser field could be helpful in allowing a wider range of J,M states to be drawn into the pendular regime. Attaining values of $\Delta\omega$ of several hundred should be feasible.

Iodine Monochloride. This molecule has become a favorite test case for orientation techniques.[23] As its polarizability anisotropy parameter is large, high values of $\Delta\omega$ are readily obtained. The pseudo-first-order effect thus can become extremely strong for a very weak static field (as in Figure 5). For example, for ICl a static field of only 10 V/cm is required to obtain $\omega = 0.002$, which for $\Delta\omega > 50$ would yield $\langle\cos\theta\rangle > 0.9$ for the 0,0 state. With such a weak field, it would become feasible to modulate it, an advantage for reaction dynamics experiments. A large polarizability anisotropy may also make feasible work with CW rather than pulsed lasers, a marked advantage for reaction studies. By use of a build-up cavity, CW fields up to 10^{10} W/cm^2 are now in prospect. For ICl, such a field would give $\Delta\omega = 8$, enough to bind well the lowest tunneling doublet. Since molecules like ICl can be cooled to quite low rotational temperatures, even $\sim$1 K, in a strong supersonic expansion, the lowest-lying states can be endowed with substantial populations.

A CW laser would also facilitate combining with static fields sequentially rather than simultaneously. For instance, a pair of static fields flanking the laser field might be employed, as in Rab's three-field method for molecular beam resonance spectroscopy.[31] The first static field could prepare an oriented pendular eigenstate, the second one could analyze whether reorientation, either by a radiation-induced transition or by tunneling through the polarizability barrier, had occurred during transit through the intervening laser region.

Hydride Molecules. It has long been considered impossible to achieve any appreciable orientation for molecules with large rotational constants, such as hydrogen chloride, since only small values of ω could be achieved. However, since for HCl it appears feasible to push the polarizability interaction up to $\Delta\omega \approx 10$, the pseudo-first-order Stark effect now provides a way to get substantial orientation (cf. Table 2). Indeed, an exceptionally high ensemble-averaged orientation can be had, since for such molecules at low temperatures most of the population resides in the 0,0 state. Such orientation can be somewhat more

readily obtained with a deuterated isotope, as its rotational constant is smaller by about a factor of two. Since the first-order $\langle\cos\theta\rangle$ increases strongly when the polarizability interaction becomes stronger, hydrogen iodide and hydrogen cyanide are quite good candidates for orientation.

NO and CO. The prospects for orienting nitric oxide and carbon monoxide (ground electronic states) are much like those for hydrogen halides; the rotational constants are less big, but the dipole moments are much smaller. Again, the polarizability interaction is large enough to make orientation by the pseudo-first-order Stark effect quite feasible. This is of particular interest in view of current work in pursuit of molecular trapping. A scheme for confining nitric oxide in a magnetic trap[32] calls for creating pendular states by use of congruent electric and magnetic fields.[17] This provides a means to separate out states susceptible to trapping, which have $\langle\cos\theta\rangle$ negative. Another scheme under development plans to slow down and eventually trap polar molecules by means of the interaction of their dipole moments with a series of pulsed electric fields.[28] The prototype employs the $a^3\Pi$ metastable excited electronic state of carbon monoxide, because it has a first-order Stark effect and a sizable dipole moment. The pseudo-first-order Stark effect may enable the ground state of CO to be used instead, despite its small dipole moment.

Other Molecules. Nitrous oxide is another example in which a small ω can be redeemed by a sizeable $\Delta\omega$ (as exemplified in Figure 5). For all the other molecules included in Table 3, the polarizability interaction is also large enough to make available a strong pseudo-first-order Stark effect.

For paramagnetic (and polarizable) molecules subjected to a static magnetic field together with a laser electric field, prospects can be assessed in analogous fashion. An advantage is that often ω-values as large as 10^3 can be reached with a static magnetic field (not limited by sparking as with an electric field). A strong pseudo-first-order Zeeman effect can thereby be obtained with appreciably smaller $\Delta\omega$-values, thus fostering use of a CW laser. Augmenting a static magnetic field with a laser field may prove useful in polarization spectroscopy of pendular molecules.[24]

The versatility gained by combining static and laser fields, briefly illustrated here, stems from melding different modes of hybridization in forming pendular states. Such melding can be extended in a variety of ways. We note just the variant simplest to implement: introducing a tilt angle β between the field directions.[33] Then in eqs 5 and 6 and elsewhere, angles θ_S,ϕ_S and θ_L,ϕ_L must be distinguished in locating the molecular axis relative to the field directions, with

$$\cos\theta_S = \cos\beta\,\cos\theta_L + \sin\beta\,\cos\theta_L\,\cos\phi_L \qquad (22)$$

Since azimuthal symmetry is lacking, the hybridization involves M as well as J-states. Also, energy levels that differ in the sign of M are no longer degenerate. As customary selection rules break down, and curve crossings run rife, the complexity of hybridization becomes downright botanical.

References and Notes

(1) Friedrich, B; Herschbach, D. *Daedalus* **1998**, *127*, 165.

(2) Rigden, J. S. *Rabi*; Basic Books: New York, 1987.

(3) Gordon, R. J.; Rice, S. A. *Ann. Rev. Phys. Chem.* **1997**, *48*, 601 and references herein.

(4) Zare, R. N. *Science* **1998**, *279*, 1875 and references therein.

(5) Dion, C. M.; Keller, A.; Atabek, O.; Bandrauk, A.D. *Phys. Rev. A.* **1999**, *59*, 1382 and references therein.

(6) Bardeen, C. J.; Yakovlev, V. V.; Wilson, K. R.; Carpenter, S. D.; Weber, P. M.; Warren, W. S. *Chem. Phys. Lett.* **1997**, *289*, 151.

(7) Assion, A.; Baumert, T.; Bergt, M.; Brixner, T.; Kiefer, B.; Seyfried, V.; Strehle, M.; Gerber, G. *Science* **1998**, *282*, 919.

(8) *J. Phys. Chem. A* **1997**, *101*, 7461−7690 (special issue on stereodynamics of chemical reactions, and references therein).

(9) As usual, here anisotropy in the spatial distribution of a molecular axis is designated *orientation* if it behaves like a single-headed arrow and *alignment* if like a double-headed arrow.

(10) Seideman, T. *J. Chem. Phys.* **1996**, *106*, 2881; **1997**, *107*, 10240.

(11) Stapelfeldt, H.; Sakai, H.; Constant, E.; Corkum, P. B. *Phys. Rev. Lett.* **1997**, *79*, 2787.

(12) Wieman, C. E.; Pritchard, D. E.; Wineland, D. J. *Rev. Mod. Phys.* **1999**, *71*, S263 and references therein.

(13) Friedrich, B.; Herschbach, D. *J. Phys Chem.* **1995**, *99*, 15686 and references therein. In eq 29 of this paper, the numerical coefficient on the right-hand side should be larger by a factor of 2.

(14) Ortigoso, J.; Rodriguez, M.; Gupta, M.; Friedrich, B. *J. Chem. Phys.***1999**, *110*, 3870.

(15) Sakia, H.; Safvan, C. P.; Larsen, J. J.; Hilligsøe, K. M.; Held, K.; Stapelfeldt, H. *J. Chem. Phys.* **1999**, *110*, 10235.

(16) Friedrich, B.; Herschbach, D. *Z. Phys. D* **1992**, *24*, 25.

(17) Friedrich, B.; Slenczka, A.; Herschbach, D. *Can. J. Phys.* **1994**, *72*, 897.

(18) Friedrich, B.; Herschbach, D. *Z. Phys. D.* **1996**, *36*, 221. Equation 20 of this paper is misprinted; it should be replaced by eq 14 of the present paper. Also, the numerical factor in eq 21 should be larger by a factor of 2.

(19) Lowan, A. N. In *Handbook of Mathematical Functions*; Abramowitz, M., Stegun, A., Eds.; Dover: New York, 1972; p 751.

(20) For example, see Townes, C. H.; Schawlow, A. L. *Microwave Spectroscopy*; McGraw-Hill: New York, 1955; pp 87 and 254.

(21) Loesch, H. J. *Ann. Revs. Phys. Chem.* **1995**, *46*, 555 and references therein.

(22) Wu, M.; Bemish, R. J.; Miller, R. E. *J. Chem. Phys.* **1994**, *101*, 9447.

(23) Gazalgette, G.; White, R.; Trénec, G.; Audouard, E.; Büchner, M.; Vigué, J. *J. Phys. Chem.* **1998**, *102*, 1098.

(24) Slenczka, A. *Chem. Eur. J.* **1999**, *5*, 1136 and references therein.

(25) Franks, K. J.; Li, H.; Kong, W. *J. Chem. Phys.* **1999**, *110*, 11779.

(26) Brooks, P. R. *J. Phys. Chem.* **1993**, *97*, 2153 and references therein.

(27) Kim, W.; Felker, P. M. *J. Chem. Phys.* **1996**, *104*, 1147; **1997**, *107*, 2193; *J. Chem. Phys.* **1998**, *108*, 6763.

(28) Jongma, R. T.; von Helden, G.; Berden, G.; Meijer, G. *Chem. Phys. Lett.* **1997**, *270*, 304. Bethlem, H. L.; Berden, G.; Meijer, G. *Phys. Rev. Lett.* **1999**, *83*, 1558.

(29) When only the total polarizability is known, we resorted to a rule of thumb: $\Delta\alpha/\alpha \approx \alpha_\perp/\alpha \approx 0.75$; these ratios hold whenever $\alpha_\parallel/\alpha_\perp = 2$ and are quite close to the average of data in ref 30 for a dozen linear molecules (omitting diatomic hydrides, for which $\Delta\alpha/\alpha \approx 0.3$).

(30) Hirschfelder, J. O.; Curtis, C. F.; Bird, R. B. *Molecular Theory of Gases and Liquids*; Wiley: New York, 1954; p 950. Also, see: *Handbook of Chemistry and Physics*, 71st ed.; The Chemical Rubber Company: Boca Raton, 1990.

(31) Ramsey, N. F. *Molecular Beams*; Oxford University Press: London, 1955; pp 298−309.

(32) Friedrich, B.; deCarvalho, R.; Kim, J.; Patterson, D.; Weinstein, J. D.; Doyle, J. M. *J. Chem. Soc., Faraday Trans.* **1998**, *94*, 1783.

(33) Friedrich, B.; Herschbach, D. *J. Chem. Phys.* **1999**, *111*, 6157.